Chapter 12
Nature of Floods in the Khari River Basin, Eastern India

Subhankar Bera and Abhay Sankar Sahu

Abstract Floods over the deltaic land of Ganga-Brahmaputra-Meghna River system made a unique fluvial landscape. This flat anastomosing landscape is developed by overtopping and deposition of alluvium in their course and has diversity in flood nature from one to other river systems. The objective of this work is to discuss the flooded nature of the Khari River Basin (KRB) and areas of active flood that can be vulnerable to society. The KRB is a small right-hand tributary of the Bhagirathi-Hugli stream of the lower Ganga River system. Geomorphic parameters of basin and drainage networks have been used and analyzed in the GIS domain. High-surface runoff and seepage are the causes of peak flow during monsoon time which creates four to five times flood every year. Active floodplain of the Khari River is the regional geomorphic low surface discontinued by geomorphic highs where channels are more sinuous. Intensive flood and wider floodplain have been observed between Palumba and Randa village that is the result of high discharge by large tributaries, draining approximately 45% of the KRB area. Human intervention in form of longitudinal discontinuation of the floodplain has made artificial damming in the natural flow direction that intensifies the flood over this region. Though this water-logged area is vulnerable for the floodtime crops, it helps in high yielding after the flood, and most settlements are located above the active floodplain.

Keywords Flood · River system · Basin morphology · Small river · Human intervention

1 Introduction

Flood is a geomorphic, meteorological, and hydrological process of a drainage basin in the plain land and in the deltaic part that alters the existing landforms. Though flood is a natural phenomenon, sometimes human activities are causes of floods. Flood is a major problem in the floodplains, areas that are often attractive for human

S. Bera (✉) · A. S. Sahu
Department of Geography, University of Kalyani, Kalyani, West Bengal, India

A. Islam et al. (eds.), *Floods in the Ganga–Brahmaputra–Meghna Delta*, Springer Geography, https://doi.org/10.1007/978-3-031-21086-0_12

developments, and in the period from 1970 to 2012, floods caused over one million deaths (WMO-World Meteorological Organization; https://public.wmo.int/en/our-mandate/water/floods, dated: 23/09/21). As reported by the WHO (World Health Organization), in between 1998 and 2017, more than 2 billion people have been affected by floods worldwide, and in the last 10 years, 80–90% of documented natural hazards are caused by floods, severe storms, and tropical cyclones (https://www.who.int/health-topics/floods#tab=tab_1, dated: 23/09/2021). Among the continents, Asia faced the average highest numbers of flood events that continually increase in the last 65 years, and in the last decade, average of 60 major floods were reported every year (Sohoulande & Singh, 2016).

Over the Indian subcontinent, the significant increasing intensity and frequency of extreme precipitation events are potential to lead the flood events, though few recent studies in monsoon show a gradual decline circulation and precipitation amount over India (Ali et al., 2019). Frequent flooding of the Gangetic West Bengal is an inherent characteristic, particularly in the western part of the Bhagirathi-Hugli River. At present, ~42.55% of the total geographical area of this state is susceptible to flood (I & W. D., Govt. of W.B., Annual Flood Report, 2020). Floods in North Bengal are causes by rivers draining in the Himalayan parts. In South Bengal, mostly rivers like Ajay, Mayurakshi, Damodar, and Kangsabati are draining the Chotanagpur plateau and finally outfall into the Bhagirathi-Hugli River and carry a huge volume of water during the monsoon season or in an event of extreme precipitation that causes floods in the Deltaic Rarh Bengal (DRB). Thus, understanding flood nature became necessary for regional development. As flood is an event in the area of drainage basin, the study of drainage characteristics or drainage basin morphometry has become a pioneer of flood analysis that is helpful in flood risk control (Odiji et al., 2021; Leopold & Miller, 1956; Leopold & Maddock, 1953).

The flood of the DRB has widely been studied in different fields focusing on the large rivers which had developed devastating hazards for the society like floods at the lower part of the Mayurakshi, Ajay, Damodar, and Dwarakeswar River Basin (Islam & Barman, 2020; Pal et al., 2020; Islam & Sarkar, 2020; Mukhopadhyay, 2010; Malik & Pal, 2021; Ghoh & Guchhait, 2016; Singh et al., 2020). The interfluves of small river basins are paid less attention because of lack of data, though these rivers are also potentially vulnerable. The Khari River Basin (KRB), which is the focused area of this study, has no research work on the basin characteristics and flood. The KRB has been first explored by Bagchi and Mukherjee (1979) and Sen (1993) in terms of geomorphic analysis of this region and later on by Singh et al. (1998), Chakarbarti and Nag (2015), Roy & Sahu (2015), Roy and Bera (2018), and Barman et al. (2018), focusing on the aspects of regional tectonics and basin, and less importance has been given to understanding these interfluves of rivers' geomorphic process and flood nature. So, the objective of this work is to discuss the flood of the KRB and the role of the drainage basin morphometry and to prepare a map of the active floods areas that are vulnerable to society. This work also will help to understand the geomorphology and hydrological characteristics of West Bengal's small alluvial rivers.

2 Study Area

The KRB is a right-hand tributary drainage of the lower Ganga River system, draining an area of 1208 km^2 of the interfluves of Ajay-Damodar Rivers of the Purba Bardhaman district, India. The Khari River is originating from the Panagarh lateritic upland (23°24′44.50″N, 87°31′58.56″E) at an altitude of ~58 meters (above MSL), near Maro village, and flows eastward ~212 km and joined with the Bhagirathi-Hugli River near the Kalna Town (23°16′4.67″N, 88°19′46.53″E) (Fig. 12.1a). Geographical extension of the studied KRB is 23°16′N to 23°32′N latitudes and 87°30′E to 88°18′E longitudes. The KRB drains the administrative area of Budbud, Galsi, Bhatar, Monteswar, Purbasthali, the northern part of Burdwan, the southern part of Katwa, and Mongalkote police stations.

Physiographically, the study basin comes under the eastern part of the "Rarh Bengal" (Bagchi & Mukherjee, 1979), and the surface geological formation of this region is mostly covered by quaternary alluviums (District resource map, GSI, 2001) (Fig. 12.1b). Geomorphologically, the KRB is an old deltaic part which belongs to the Damodar para-delta (Singh et al., 1998). Bagchi & Mukherjee (1979) divided the major relief characteristics of this area into three physiographical units that are marked by the counters of 18 m and 36 m, respectively (Roy & Sahu, 2015) (Fig. 12.1a). The climatic condition of the area is tropical wet and dry (aw) in

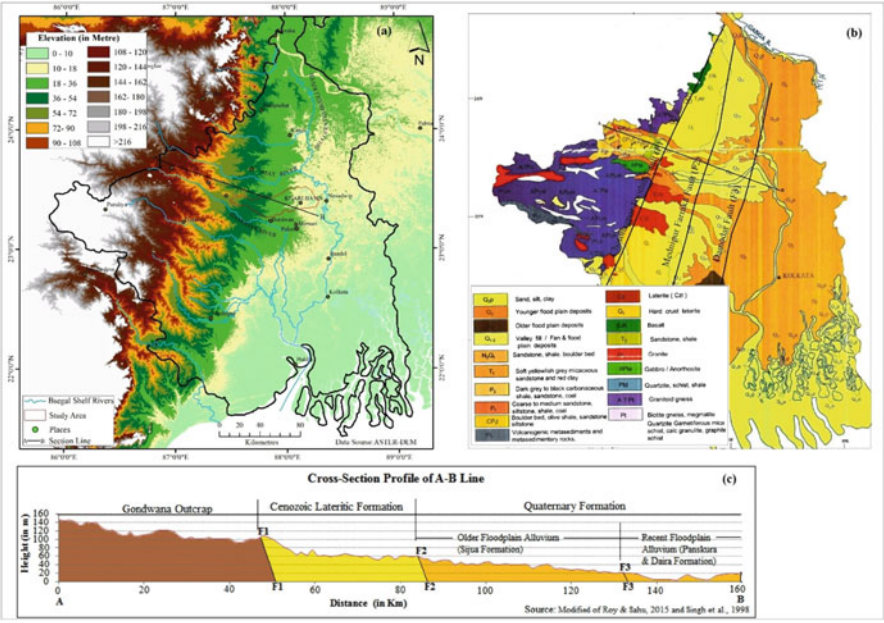

Fig. 12.1 Location map of the study area. (**a**) Elevation map of the study area and the surroundings, (**b**) surface geology of the South West Bengal and study area with major faults, and (**c**) cross section of the surface geology along the A-B represents the surface slope and surface formation

types controlled by the seasonal migration of tropic of cancer (23°0.30′N). Mean annual temperature of the region is ~26.3 °C and receives more than 100 mm mean annual rainfall, and approximately 80% of the total precipitation goes on in the monsoon months with an average of 350 mm. Though the Khari River is mainly rain-fed, bankfull discharge is observed during the monsoon period or torrential rainfall of depression that developed floods.

3 Database and Methodology

The main data used in this work is ASTER Global DEM (Advance Spaceborne Thermal Emission and Reflection Radiometer, spatial resolution of 30 m), and heights that were obtained from the Survey of India topographical maps (79A/3& 79A/7 of 1:50,000 scale) have been wont to develop the surface elevation map (SEM) in ArcGIS. Finally, the SEM database has been applied to compute the basin aerial and relief morphometric data by dividing the basin into 1 km^2 grids. The KRB drainage network (Fig. 12.2) has been digitized from the "aerial Bing map"(spatial resolution view of 0.30–0.33 m) through QGIS "OpenLayer Plug-in tool" and delineated after Strahler's classification (1964), which were used for the analysis of linear morphometry of the basin. The KRB has also been delineated into 17 sub-basins and named as A to Q for the detailed analysis of flood potentiality (Fig. 12.2). The surface runoff dominates sub-basins D and N, Q has no tributary, and the paleochannels have dominated M. Therefore, these sub-basins themselves are areas of water logging. A total of 16 parameters (Table 12.1) have been used for the drainage network and basin morphometric analysis which are grouped into (a) linear parameters, (b) aerial parameters, and (iii) relief parameters. A correlation has been run between the 16 parameters to look at the association among them (Fig. 12.3).

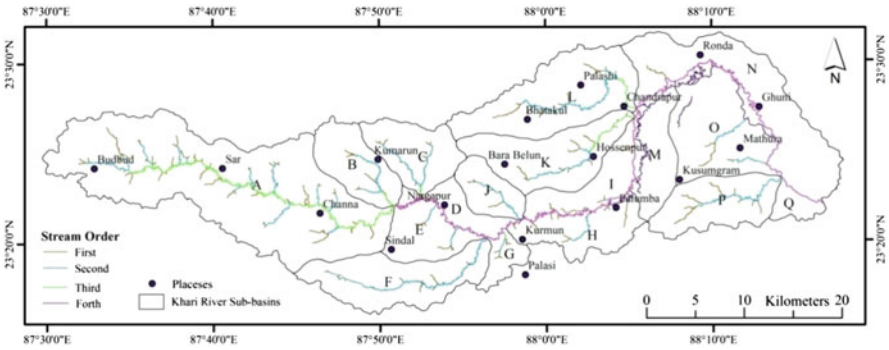

Fig. 12.2 KRB sub-basins and the drainage hierarchy

Table 12.1 Morphometric parameters used to evaluate the KRB flood

Aspect of analysis	Morphometric parameters	Equation/formula	Followed by	Remarks
Linear aspect	Stream order (u)	Stream hierarchy	Strahler (1964)	The higher the order are, the more potential of hydraulic efficiency.
	Stream number (nu)	Nu ¼ N1þN2þ . . . Nn	Horton (1945)	Comparative assessment of stream number shows surface runoff and channelized flow of water.
	Stream length ratio (S_{tr})	$S_{tr} = L_u / L_{u-1}$	Horton (1945)	Shows the evolution of the geomorphic streams that can be related to hydraulic efficiency.
	Bifurcation ratio (R_b)	$R_b = N_u / N_{u-1}$	Schumm (1956)	R_b normally ranges between 3.0 and 5.0 which indicate natural drainage system of homogenous surface, and the higher or lower values indicate the irregularities in drainage basin evolution with varied lithological and structural controls.
	Mean bifurcation ratio (B_R)	B_R = average of R_b	Strahler (1957)	
	Stream gradient ratio (S_g)	$S_g = (a\text{-}b)/l$	Sreedevi et al., (2005)	Higher the S_g is steep slope, and lower values of S_g are gentle slope, which indicates the stream power and discharge potentiality of individual stream.
Aerial aspect	Stream frequency (S_f)	$S_f = \sum N_u / A$ (no./k^2)	Horton (1945)	Shows the flow concentration of unit area of watershed to runoff processes.
	Drainage density (D_d)	$D_d = \sum L_u / A$ (km/km^2)	Horton (1945)	Higher density is largely associated with floods in lower basin part.
	Form factor (F_f)	$F_f = A/L^2$	Horton (1945)	The value 0.786 is a circular basin, and lover values (<0.5) shows narrow and elongated watershed that are more vulnerable to flood.
	Elongation ratio (E_r)	$E_r = 1.128\sqrt{(A/L)}$	Schumm (1956)	Shows the shape of the basin, circular (0.9–1.0), oval (0.8–0.9), less elongated (0.7–0.8), elongated (0.5–0.7), and more elongated (<0.5) that are linked with runoff potentiality.
	Circularity ratio (C_r)	$C_r = 4paiA/P^2$	Strahler (1957)	Identify the circularity of the basin. Lower values (<1) indicate elongated form and runoff generation.
	Compactness coefficient (C_c)	$C_c = 0.2821$ $P/A^{0.5}$	Gravelius (1914)	Is the ratio between the perimeter of the basin and the circumference of a circle; that area is equal to basin and used for inter-basin comparison.

(continued)

Table 12.1 (continued)

Aspect of analysis	Morphometric parameters	Equation/formula	Followed by	Remarks
	Constant of channel maintenance (C_m)	$C_m = 1/D_d$	Schumm (1956)	Shows the dynamic equilibrium nature of basin and comprises an important channelized flow indicator.
	Length of overland flow (L_o)	$L_o = 1/2\ D_d$	Horton (1945)	Shows the hydrological and physiographic condition of basins.
Relief aspect	Relative relief (R_r)	$R_r = B_r / L$	Schumm (1956)	Value >0.5 indicates high relative relief areas and < 0.5 shows low relative relief that are linked with basin surface slope.
	Absolute relief (A_r)	$A_r = H\text{-}h$	Schumm (1961)	Indicates the unit gradient distribution which helps to interpret runoff potentiality.

4 Result and Discussion

The KRB is an elongated fourth-order drainage basin of 1 fourth-order stream, 6 third-order stream, 33 second- order streams, and 157first-order streams, and the width of the basin increases downstream from about 8.5 km to ~17 km. Though both sides of the trunk river are drained by an equal number of sub-basins, the number of left-side streams is almost double than the right side, and the gradient of the streams are steeper than the right side (Table 12.2). Total length of the stream is ~537 km with the drainage density of ~0.44 km/km^2, where first, second, third, and fourth order contribute almost 27%, 36%, 17%, and 20%, respectively, of the total length. The total length and the area of the left-side drainage basins are also greater than the opposite side. Sub-basin variations of the stream order, number, and stream length are given in Table 12.2. Though these three have no direct relation in peak flood generation, it has a positive relation with surface runoff generation that developed flood (Nageswara Rao, 2020). The mean bifurcation ratio of the KRB is $B_r = 5.42$, that is, higher than any other small rivers draining at the Ajay-Damodar interfluves (Roy & Sahu, 2015), and B_r between first, second, secondto third, and third to fourth orders are 4.80, 5.50, and 6.00, respectively. Sub-basins *Br* ranges from 2 to 13 (Table 12.3). A negative exponential trend has been observed between the stream number and stream orders (Fig. 12.4), indicating the natural extension of the network (Horton, 1945). The left side basin area is drained by higher Nuand by the stream length that exhibits the area of potential for surface runoff (Resmi et al., 2019). The sub-basin A is draining by the highest Nu of 70 and L_u of ~154 km (Table 12.2). Sub-basins C, B, H, F, L, and K are draining by relatively higher Nu (>10), and sub-basin O, I, G, J, P, and E are associated with the lower value of Nu (<10) (Table 12.2). First- and second-order average stream lengths are very high in

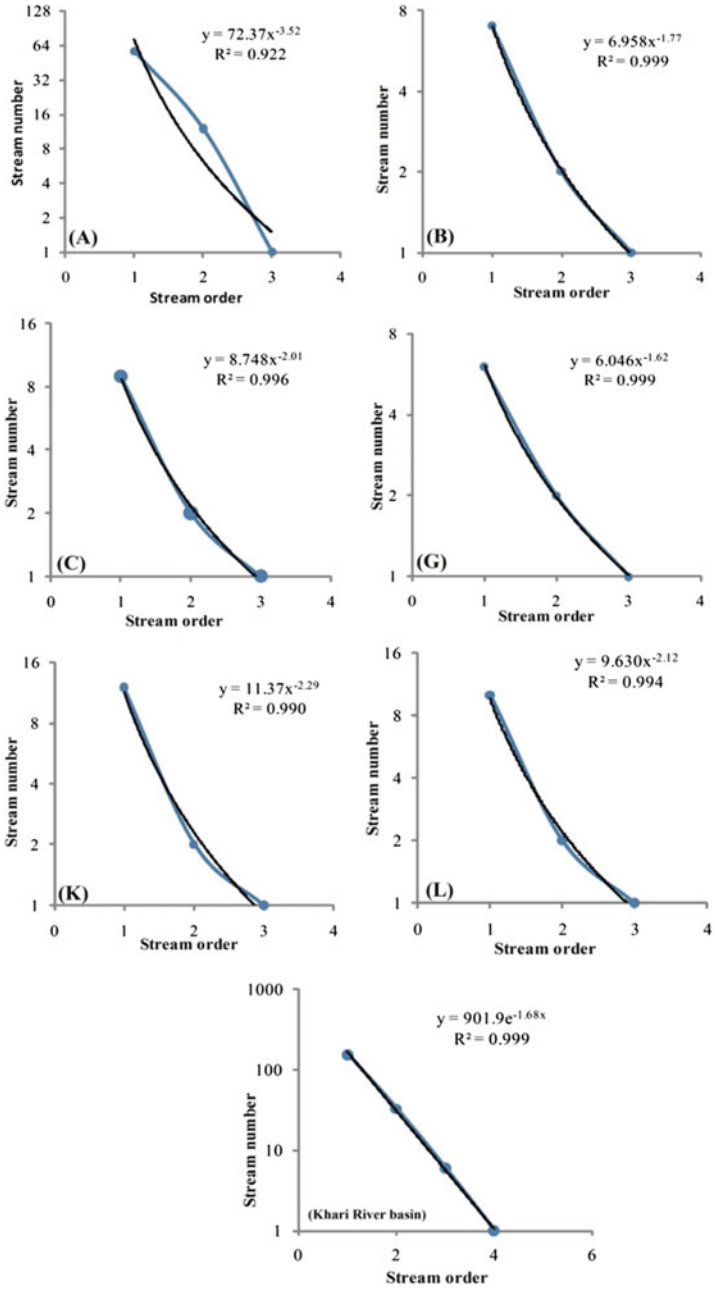

Fig. 12.3 Semilogarithmic diagram of stream numbers versus stream orders of the KRB and sub-basins A, B, C, G, K, and L, respectively. Regression coefficient curve values are indicated

Table 12.2 Basin properties of the KRB sub-basins

Sub-basin name	Stream order (u)	Total stream number of the u order (Nu)				A = Area of the basin (km^2)	L_u = Total stream length of the order u (km)				L = Basin max length (km)	P = Perimeter (Km)	H = Maxelevation (m)	h = Minelevation (m)	a = Stream elevation at source (m)	b = Stream elevation at confluence (m)	l = Actual stream length (km)	Straight line stream length (km)	Average stream gradient (m/km)
		1st	2nd	3rd	Total		1st	2nd	3rd	Total									
A	3	57	12	1	70	295.34	45.56	40.52	67	153.06	34.96	106.40	73	27	58.70	29.50	47.63	32.54	0.613
B	3	7	2	1	10	48.68	5.71	12.33	3.85	21.89	10.89	30.03	56	29	41.20	30.00	14.89	7.56	0.752
C	3	9	2	1	12	51.53	3.80	16.28	2.39	22.47	9.86	31.41	45	25	38.00	26.20	12.42	7.03	0.95
D	1	1	–	–	1	25.31	0.45	–	–	0.45	8.00	49.35	34	19	26.30	24.50	0.45	0.40	4.50
E	2	6	2	–	8	41.59	4.41	6.9	–	11.31	7.75	40.31	36	20	30.4	20.6	5.9	2.9	1.16
F	2	13	1	–	14	82.13	6.68	31.18	–	37.86	20.2	52.16	41	20	37.3	20	31.22	16.91	0.554
G	3	6	2	1	9	16.55	3.27	2.64	1.22	7.13	6.75	23.43	29	20	27.9	21.6	4.24	2.83	1.48
H	2	9	2	–	11	50.79	10.24	7.34	–	17.58	8.65	51.16	28	15	25.6	13.4	6.34	4.16	1.92
I	2	5	1	–	6	41.65	8.19	0.69	–	8.88	12.5	53.32	25	13	15.3	13.2	1.69	1.31	1.24
J	2	5	1	–	6	29.55	4.35	10.31	–	14.66	8.5	22.37	34	19	31	19.5	11.16	6.81	1.03
K	3	12	2	1	15	78.7	11.52	13.98	9.1	34.6	17.71	45.29	33	13	26.6	12.5	23.76	12.95	0.593
L	3	10	2	1	13	107.82	13.65	24.55	5.9	44.1	19.26	53.9	34	12	30.7	11.8	32.21	14.76	0.586
M	–	–	–	–	–	48.24	–	–	–	–	12.25	40.3	20	12	–	–	–	–	–
N	1	1	–	–	1	120.66	3.5	–	–	3.5042	25.0	90.86	20	9	15.4	10.6	3.5	2.41	1.37
O	2	4	2	–	6	96.45	6.39	10.87	–	17.26	12.1	52.89	16	8	17.6	9.4	7.67	6.8	1.07
P	2	8	1	–	9	60.66	14.61	17.2	–	31.81	15.27	36.96	19	8	17.3	8	20.84	11.96	0.446
Q	–	–	–	–	–	13.11	–	–	–	–	4.93	18.41	15	9	–	–	–	–	–

Based on: Computed by authors

Sub-basin in blue color is head water basin at the western side. The sub-basins highlighted in green color are draining the left side of the KRB, and the right-side sub-basins are marked by the brown color. Dotted in place of values are not applicable for respective parameters or basins

Table 12.3 KRB sub-basins linear morphometric parameters

Sub-basin name	Stream order	Total stream number of u order				average stream length of order u (km)			Stream length ratio (S_{tr})			Mean bifurcation ratio (B_R)	Stream gradient ratio (S_g)
		1st	2nd	3rd	Total	1st	2nd	3rd	1st to 2nd	2nd to 3rd	Average		
A	03	57	12	01	70	0.80	5.58	66.98	1.124	0.605	0.865	8.38	0.613
B	03	07	02	01	10	0.82	6.17	3.85	0.463	3.203	1.830	2.75	0.752
C	03	09	02	01	12	0.42	8.14	2.39	0.233	6.778	3.505	3.25	0.950
E	02	06	02	–	08	0.74	3.45	–	0.639	–	0.639	03	0.567
F	02	13	01	–	14	0.52	31.80	–	0.214	–	0.214	13	0.554
G	03	06	02	01	09	0.55	1.32	1.22	1.239	2.164	1.777	2.50	1.480
H	02	09	02	–	11	1.34	3.67	–	1.395	–	1.395	4.50	0.585
I	02	05	01	–	06	1.64	0.69	–	11.869	–	11.869	05	0.436
J	02	05	01	–	06	0.87	10.31	–	0.422	–	0.422	05	1.030
K	03	12	02	01	15	0.96	6.99	9.10	0.824	1.536	1.180	04	0.593
L	03	10	02	01	13	1.37	12.28	5.90	0.556	4.161	2.235	3.50	0.586
O	02	04	02	–	06	1.60	5.44	–	0.587	–	0.587	02	0.432
P	02	08	01	–	09	1.83	17.20	–	0.849	–	0.849	08	0.446

Based on: Computed by authors

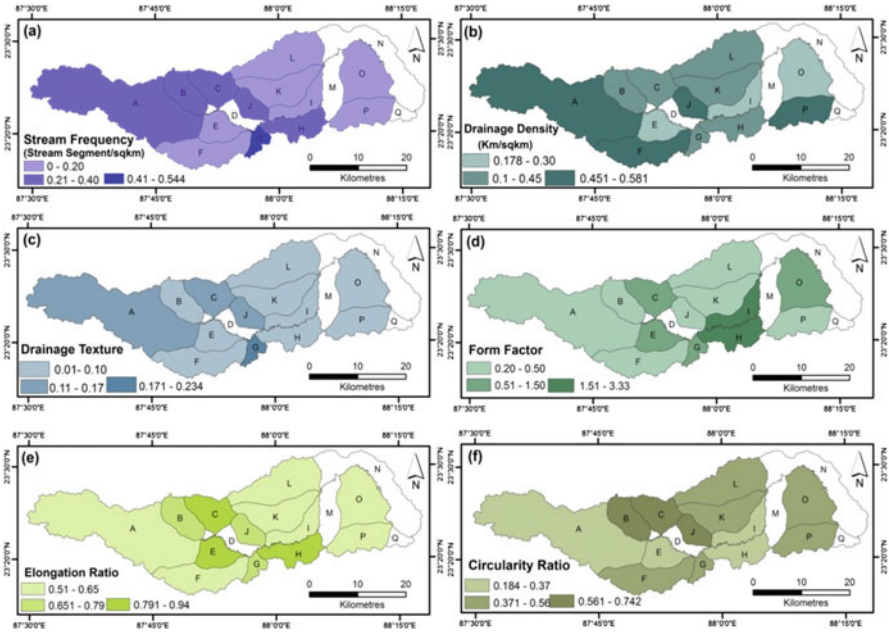

Fig. 12.4 Sub-basin wise distributions of (**a**) stream frequency (S_f), (**b**) drainage density (D_d), (**c**) drainage texture (D_t), (**d**) form factor (F_f), (**e**) elongation ratio (E_r), and (**f**) circulatory ratio (C_r)in the KRB

sub-basins K, H, J, I, P, O, L (>1 km) and in sub-basins J, F, C, L, P, K (>7 km), respectively (Table 12.2). Str values of the sub-basins P, J, L, and K are comparatively higher because of the relatively faster channel elongation process which causes the high stream gradient with channelized flow (Resmi et al., 2019) that shows diverseness between sub-basins gradient, different erosional stages, and potentiality for the surface-runoff generation. The B_R of the left-side sub-basins is comparatively high than right-side sub-basins (Table 12.3). These higher B_R and S_g of these downstream sub-basins also indicate the high discharge potentiality of tributaries to the Khari trunk stream, and high discharge into the trunk stream in the rainy season is a normal event that leads to floods over the region.

The KRB's maximum length is 82 km, and maximum width is approximately 22 km, i.e., the basin is almost 3.75 times longer, though the KRB is narrowly elongated ($E_r = 0.48$ and $F_f = 0.18$) and the basin is wider in its downstream. This is probably because of the relatively large sub-basins of the KRB draining in this part (Fig. 12.2). These sub-basins are joining with the trunk stream within a specific stretch, and their combined discharge makes the trunk stream overtopping in its floodplain. The sub-basins joining into this reach are also elongated in nature (Fig. 12.4d–f) indicating more surface runoff because the shape also controls the rate of flow at which it discharged into the trunk channels (Fenta et al., 2017). According to Thomas et al. (2012), elongated-shaped watersheds can be marked by a

flat hydrograph of longer duration with gentle rising and recession limbs. However, a more elongated watershed is more efficient in discharge of runoff; the hydrological response has also been affected by several factors like LULC, basin gradient, soil type, or rainfall intensity. The correlation shows that the F_f and E_r have C_c, C_m, and L_o and also have a positive relationship with the relief aspects of the basin (Table 12.4).

The spatial variation of the S_f, D_d, and D_t indicates the landscape dissection by the stream network along with the parameters of C_c and L_o. These are important linear variables that are related to the hydrological properties of the drainage system and help to predict the runoff and sediment yield (Fenta et al., 2017). The computed D_d of the KRB is 0.44 km/km^2 (Fig. 12.6d) and ranges between 0.18 and 0.58 km/km^2 (Fig. 12.4b). Though, the overall D_d is very low, sub-basins J, P, and A D_d values are relatively high ($D_d > 0.5$), and sub-basins F, B, K, G, and C values are near to this (Fig. 12.4b). According to Ramalingam and Santhakumar (2001), the low D_d indicates less channelized flow which is a result of the higher infiltration rate caused by alluvium surface and higher-surface runoff. The S_f value of the KRB is ~0.17 no./km^2, which ranges between 0.06 and 0.54 no./km2 (Fig. 12.4a). Relatively moderate values of S_f have been observed at the middle part of the KRB which also indicates the possibility to generate surface runoff. Moreover, in sub-basin-wise analysis (Fig. 12.4a), S_f values are relatively higher in sub-basin C, B, J, K, P, and L indicating a high rate of channelized flow. Normally, when surface permeability decreases, runoff increases, and as a result of it, numbers of channels developed and thus tend to be relatively higher S_f. In the correlation matrix, S_f, D_d, and D_t showed negative or very low positive correlation with other aerial and relief aspects (Table 12.4). Figure 12.5b shows the sub-basins draining the downstream part have much similarities.

The C_m and L_o are another two important aerial aspects from the hydrological perspective as proxy indicators of the dynamic equilibrium stage of the river basin (Schumm, 1956) and the length that water must travel before discharging into the channel, i.e., the greater the L_o, the greater is the possibility of infiltration and lesser the surface runoff (Horton, 1945). For the KRB, the calculated value of C_m and L_o are 2.27 and 0.262 km, respectively. And the sub-basins ranges $C_m = 1.721$ to 5.617 and $L_o = 0.861$ to 2.809, respectively (Fig. 12.5d). According to Ngapna et al. (2018), such values are normally associated with the low-energy surface and its hydrology controlled by a humid environment. Thomas et al. (2012) interpreted shorter L_o values as characteristics of areas with steeper basin gradient that generate high-surface runoff. Lower values of L_o for sub-basins A, F, J, and P indicate more surface-runoff generation and moderate values of L_o for sub-basins B, C, K, L, H, E, and G moderate type of surface-runoff generation (Fig. 12.5d). The correlation analysis showed L_o and C_m are statistically significant and positively correlated and have a significant inverse relationship between the D_t and D_d. So in sub-basins with lower drainage density, L_o is high which generates more surface runoff and that leads to the possibility of flood at the KRB downstream part.

To synthesize the hydraulic nature of landform and characteristic of the overland flow of the basin, quantitative investigation of the relief aspect is the base of this

Table 12.4 Correlation matrix of selected morphometric parameters of the KRB sub-basins

	B_r	S_{tr}	S_g	Sf	D_d	D_t	F_f	E_r	C_r	C_c	C_m	R_r	A_r	L_o
B_r	1													
S_{tr}	−0.136	1												
S_g	−0.299	−0.144	1											
Sf	−0.155	−0.081	0.873[b]	1										
D_d	0.463	−0.445	0.364	0.312	1									
D_t	0.016	−0.239	0.867[b]	0.937[b]	0.599[a]	1								
F_f	−0.190	0.778[b]	−0.205	−0.059	−0.603[a]	−0.293	1							
E_r	−0.624[a]	−0.183	0.071	−0.039	−0.505	−0.204	0.634[a]	1						
C_r	−0.158	−0.376	0.340	−0.046	0.517[a]	0.152	−0.614[a]	0.003	1					
C_c	0.112	0.590[a]	−0.330	0.003	−0.537	−0.203	0.811[b]	0.015	−0.948[b]	1				
C_m	−0.396	0.421	−0.414	−0.401	−0.947[b]	−0.620[a]	0.536	0.453	−0.460	0.489	1			
R_r	−0.339	0.581[a]	0.213	0.193	−0.246	0.020	0.661[a]	0.392	−0.088	0.300	0.108	1		
A_r	−0.015	0.229	−0.314	−0.288	−0.105	−0.268	0.044	0.006	−0.137	0.145	0.098	0.336	1	
L_o	−0.395	0.421	−0.414	−0.401	−0.947[b]	−0.620[a]	0.535	0.453	−0.460	0.489	1.000[b]	0.108	0.098	1

Based on: Computed by authors

[a]Marks correlation is significant at the 0.05 level (2-tailed)

[b]Marks correlation is significant at the 0.01 level (2-tailed)

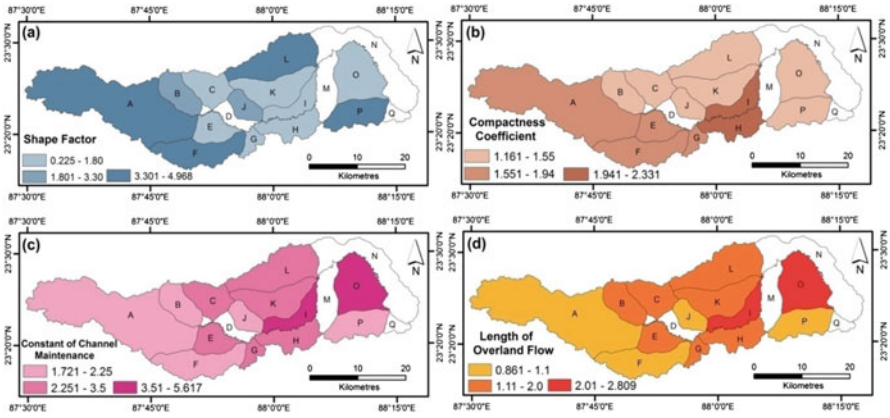

Fig. 12.5 Sub-basin-wise distributions of (**a**) shape factor, (**b**) compactness coefficient (C_c), (**c**) constant of channel maintenance (C_m), (**d**) length of overland flow (L_o) in the KRB

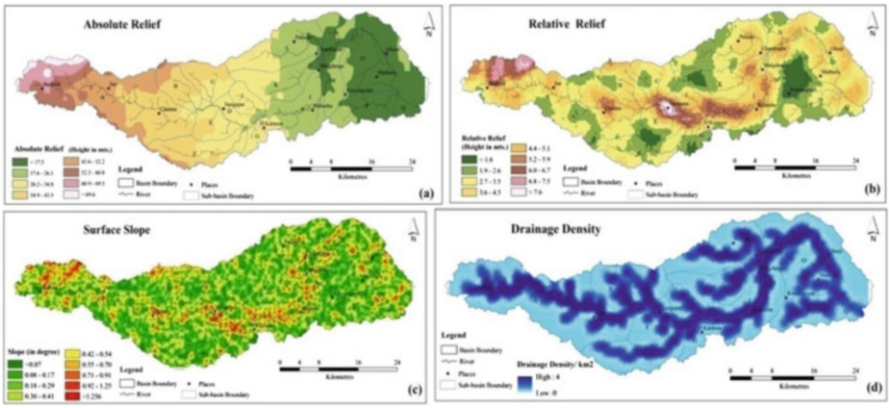

Fig. 12.6 Spatial distribution of morphometric attributes of the KRB, (**a**) absolute relief (A_r), (**b**) relative relief (R_r), (**c**) surface slope (S), and (**d**) drainage density (D_d)

(Fenta et al., 2017). In this work, the absolute relief (A_r), the relative relief (R_r), and the surface slope parameters of the basin have been interpreted to reveal the nature of surface runoff. The total relief of the KRB is 69 m, and the basin length is 81.9 km, i.e., the basin surface gradient is 0.84 m/km. This is a moderate gradient surface above the base level of the Khari River with moderate potential energy to move water down the slope. Distribution of the A_r value indicates that the basin is sloped from west to east and rivers are flowing according to the slope (Fig. 12.6a). Higher A_r values at the western part of the basin are related with the potential energy of surface runoff in this area. Figure 12.6c also shows that this part's surface slope is relatively moderate to high. According to Thomas et al. (2012), comparatively high A_r values show steep sloping and higher-energy gradient surface area, which has been

manifested as a high-surface runoff area (Fenta et al., 2017). The A_r and surface slope values are low at the eastern side of the basin, which is a relatively more flat surface and has less potential energy to generate surface runoff and has higher possibilities to stay water in this basin part (Fig. 12.6a).

The values of relative relief (R_r) ranges between 1.1 m and 8.40 m (Fig. 12.6b) with basin average of 2.1 covering about half of the basin. Figure 12.6b shows that the downstream area is characterized by very low relief, in particular, sub-basins K, O, F, P, E, and L which are plain surfaces with alternative picks of high R_r along the Khari mainstream. The lower values of R_r for the KRB are associated with first and second-order streams at the irrespective upstream parts (Fig. 12.6b). An area of high $R_r > 6.0$, which has been marked at the NW corner of the KRB, is an area of the dissected lateritic surface, but the higher R_r along the trunk river course, particularly near the Channa village and downstream of Nargapur village, indicates that these parts are relatively lower and potentially active floodplain areas (Fig. 12.6b). Every year during the flood event, the surface runoff that has been generated at the upper area of the sub-basins is accumulating in these areas and submerged multiple times (Fig. 12.8a–c). The slope deformation along the riverbank in this part of the river course also reveals the flooded areas (Fig. 12.6c). Though the surface slope of the basin is eastward, due to trunk stream abrupt deflection toward the north near the Palumba village and its downstream circular flow, the floodplain in this area is bounded by two-side relatively high ground of potentially high-runoff areas (Figs. 12.6b and 12.7a). The low relative relief or geomorphic high of the Kusumgram area acts as a natural barrier of the floodwater flow toward the east,

Fig. 12.7 Flood inundation and waterlodgging areas of the KBR near (**a**, **b**) Channa village and downstream of Channa village, (**c**) downstream of Nargapur village, and (**d**) the left bank area between Malumba and Chandrapur village

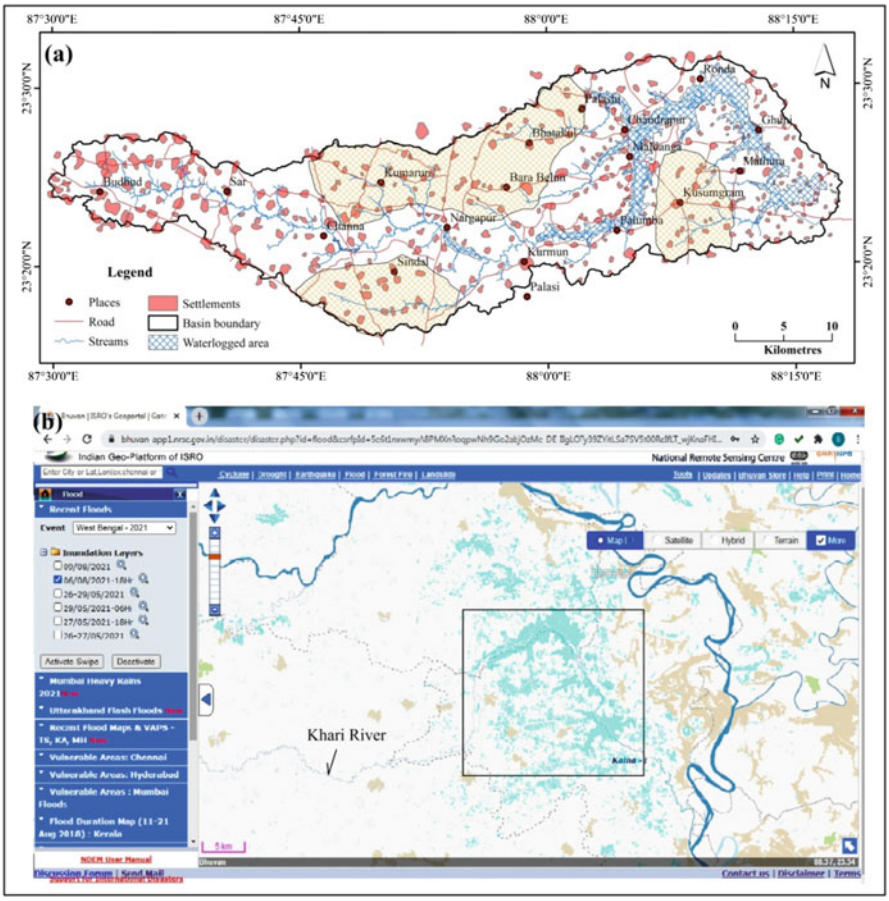

Fig. 12.8 (**a**) Areas of flood waterlogged in the KRB along with the location of settlements areas and distribution of roads. The settlements are located away from the flood waterlogged areas. Marked areas by brown color lines are the areas of potential surface of runoff. (**b**) Flood inundation area of the lower KRB during the flood event on 06-08-2021 by a catastrophic rainfall (onscreen visualization of flood data by Bhuvan, Govt. of India)

and an extensive elongated submerged or waterlogged area evolved during the floodtime (Figs. 12.7a, b and 12.8d). It is an area of about 97 km^2 waterlogging. Human intervention in form of longitudinal discontinuation of the floodplain by roads intensifies the flood and waterlogging condition in this area. Though a number of roads were disconnected and damaged by floodwater, as settlements are located above the floodplain, no one settlement is affected by flood (Fig. 12.7a). Near the Channa and Nargapur village, approximately 0.62 km^2 and 3.0 km^2 area flooded along the river, respectively. In these areas, the settlements are also located away from the present floodplain and not vulnerable to flood submergence (Fig. 12.7a).

5 Conclusion

Flood in the KRB is a response to catastrophic rainfall, as it is mainly a seasonal river that generates high-surface runoff governed by morphometric parameters of the basin and drainage. Applied parameters indicate the different degrees of correlation among them and give an overall view of the hydraulic nature of the KRB. The nature of the relief aspects and surface-slope distribution show that active floodplain of the Khari River is the regional geomorphic low surface discontinued by geomorphic highs. KRB linear and aerial aspects reveals that the sub-basins J, L, K, O, P, and H are relatively high potential areas of surface runoff that drain approximately 45% of the total basin area. The combined discharge of these sub-basins into a particular reach of the lower Khari River between Palumba and Randavillage evolved the part as a flood basin. It is an elongated and circular waterlogged area bounded by two-side geomorphic high-surface areas. Another two active floodplain and water-logged areas are developed near the Channa village and downstream of Nargapur village. Though these areas are potential for flood vulnerability and are submerged every year, as the settlements are located away from the present floodplain, the flood is not hazardous for the humans living in the basin. It will not be really possible to control flood frequency and situation in the lower part of the basin, but if we take a few constructive measures, flood vulnerability can be reduced, and for that we would recommend:

(i) We can construct more capable underpass for floodwater in lateral roads that are blocking the flow of the surface runoff in floodplain area.
(ii) As the flooded downstream area is relatively low-relief longitudinal basin, sedimentation is a common factor leading to the decreasing carrying capacity of the main channel than its middle part. So, to maintain its capacity, we need to rejuvenate the lower part.
(iii) Another possible way is diverting the floodwater through the trunk stream of the sub-basin P, as source of this stream is near to the Khari main channel near the Palumba village that have to do by an artificial channel in a controlled way. Otherwise, the Khari segment between Palumba and Mahata village may dry out due to lack of water in channel.

Acknowledgements For this work, the authors would like to convey their gratitude to the Survey of India (SoI), the Geological Survey of India (GSI, Govt. of India), and USGS for maps and also to the software (ArcGIS, QGIS, and SPSS) manufacturers for making this beautiful software used in this work. The work is supported by the Kalyani University, Department of Geography. The authors would like to thank the editors and reviewers for their constructive queries, comments, and recommendations.

References

Ali, H., Modi, P., & Mishra, V. (2019). Increased flood risk in Indian sub-continent under the warming climate. *Weather and Climate Extremes, 25*, 100212. https://doi.org/10.1016/j.wace.2019.100212

ASTER Global DEM (1arc). (n.d.). U.S. Geological Survey, https://earthexplorer.usgs.gov/

Bagchi, K., & Mukherjee, K. N. (1979). *Diagnostic survey of Rarh Bengal, part -I, morphology, drainage and flood: 1978* (1st ed.). Department of Geography, University of Calcutta.

Barman, S. D., Islam, A., Das, B. C., Mandal, S., & Pal, S. C. (2018). Imprints of new tectonism in the evolutionary record along the course of Khari River in Damodar fan delta of Lower Ganga basin. In B. C. Das, S. Ghosh, & A. Islam (Eds.), *Quaternary geomorphology in India – Case studies from the Lower Ganga basin* (pp. 105–126). Springer International Publishing. https://doi.org/10.1007/978-3-319-90427-6_6

Chakrabarti, P., & Nag, S. (2015). *Rivers of West Bengal: Changing scenario*. Department of Science and Technology, Government of West Bengal.

Fenta, A. A., Yasuda, H., Shimizu, K., Haregeweyn, N., & Woldearegay, K. (2017). Quantitative analysis and implications of drainage morphometry of the Agula watershed in the semi-arid northern Ethiopia. *Applied Water Science, 7*, 3825–3840. https://doi.org/10.1007/s13201-017-0534-4

Ghoh, S., & Guchhait, S. K. (2016). *Dam-induced changes in flood hydrology and flood frequencyof tropical river: A study in Damodar River of West Bengal*. Arab J Geosci. https://doi.org/10.1007/s12517-015-2046-6

Gravelius H (1914) Flusskunde. Goschen Verlagshan dlung Berlin. In: Zavoianu I (ed) Morphometry of drainage basins. Elsevier, Amsterdam

Horton, R. E. (1945). Erosional development of streams and their drainage basins; hydrophysical approach to quantitative morphology. *Geological Society of America Bulletin, 56*(3), 275–370.

Islam, A., & Deb Barman, S. (2020). Drainage basin morphometry and evaluating its role on flood-inducing capacity of tributary basins of Mayurakshi River, India. *SN Applied Sciences, 2*, 1087. https://doi.org/10.1007/s42452-020-2839-4

Islam, A., & Sarkar, B. (2020). Analysing flood history and simulating the nature of future floods using Gumbel method and Log-Pearson type III: The case of the Mayurakshi River basin, India. *Bulletin of Geography. Physical Geography Series, 19*(1), 43–69. https://doi.org/10.2478/bgeo-2020-0009

Leopold, L. B., & Maddock, T. (1953). *The hydraulic geometry of stream channels and some hysiographic implications* (Vol. 252). US Government Printing Office.

Leopold, L. B., & Miller, J. P. (1956). Ephemeral streams—Hydraulic factors and their relation to the drainage net. *U.S. Geological Survey, 282*, 1–37.

Malik, S., & Pal, S. C. (2021). Potential flood frequency analysis and susceptibility mapping using CMIP5 of MIROC5 and HEC-RAS model: A case study of lower Dwarkeswar River, Eastern India. *SN Applied Sciences, 3*, 31. https://doi.org/10.1007/s42452-020-04104-z

Mukhopadhyay, S. (2010). A geo-environmental assessment of flood dynamics in lower Ajoy River inducing sand splay problem in eastern India. *Ethiopian Journal of Environmental Studies and Management, 3*(2), 96–110.

Nageswara Rao, K. (2020). Analysis of surface runoff potential in ungauged basin using basin parameters and SCS-CN method. *Applied Water Science, 10*, 47. https://doi.org/10.1007/s13201-019-1129-z

Ngapna, M. N., Owona, S., Owono, F. M., Mpesse, J. E., Youmen, D., Lissom, J., Ondoa, J. M., & Ekodeck, G. E. (2018). Tectonic, lithology and climatic controls of morphometric parameters of the Edea – Eseka region (SW Cameroon, Central Africa): Implication on equatorial rivers and landforms. *Journal of Africal Earth Science, 138*, 219–232.

Odiji, C. A., Aderoju, O. M., Eta, J. B., Shehu, I., Mai-Bukar, A., & Onuoha, H. (2021). Morphometric analysis and prioritization of upper Benue River watershed. *Northern Nigeria. Applied Water Science, 11*, 41. https://doi.org/10.1007/s13201-021-01364-x

Pal, S., Mahato, S., & Bala, G. (2020). Hydro-geomorphic consequences of avulsion susceptible zones along lower Mayurakshi river of eastern India. *Remote Sensing Applications: Society and Environment, 100425*. https://doi.org/10.1016/j.rsase.2020.100425

Ramalingam, M., & Santhakumar, A. R. (2001). Case study on artificial recharge using remote sensing and GIS. Retrieved from www.GISdevelopment.net

Resmi, M. R., Babeesh, C., & Hema, A. (2019). Quantitative analysis of the drainage and morphometric characteristics of the Palar River basin, Southern Peninsular India; using bAd calculator (bearing azimuth and drainage) and GIS, Geology, Ecology, and Landscapes, 3:4, 295–307, https://doi.org/10.1080/24749508.2018.1563750

Roy, S., & Bera, S. (2018). Geophysical control on the channel pattern adjustment in the Kunur River basin of Western part of lower Ganga Basin. In B. C. Das, S. Ghosh, & A. Islam (Eds.), *Quaternary geomorphology in India – Case studies from the lower ganga basin* (pp. 89–102). Springer International Publishing. https://doi.org/10.1007/978-3-319-90427-6_5

Roy, S., & Sahu, A. S. (2015). Quaternary tectonic control on channel morphology over sedimentary lowland: A case study in the Ajay-Damodar interfluve of eastern India. *Geoscience Frontiers, 6*(6), 927–946. https://doi.org/10.1016/j.gsf.2015.04.001

Schumm, S. A. (1956). Evolution of drainage systems and slope in badlands at Perth Amboy, New Jersey. *Geological Society of American Bulletin, 67*, 597–646.

Sen, P. K. (1993). *Geomorphological analysis of drainage basin (an introduction to morphometry and hydrological parameters)*. The University of Burdwan.

Singh, L. P., Parkash, B., & Singhvi, A. K. (1998). Evolution of the lower gangetic plain landforms and soils in West Bengal, India. *Catena, 33*, 75–104. https://doi.org/10.1016/S0341-8162(98)00066-6

Singh, R. K., Vasanta Govind, K. V., Pasupuleti, S., & Nune, R. (2020). Hydrodynamic modeling for identifying flood vulnerability zones in lower Damodar River of eastern India. *Ain Shams Engineering Journal, S2090447920300137*. https://doi.org/10.1016/j.asej.2020.01.01

Sohoulande, D. D. C., & Singh, V. P. (2016). Impact of climate change on the hydrologic cycle and implications for society. *Environment and Social Psychology, 1*(1), 36–49. https://doi.org/10.18063/ESP.2016.01.002

Sreedevi, P. D., Subrahmanyam, K., & Ahmed, S. (2005). The significance of morphometric analysis for obtaining groundwater potential zones in a structurally controlled terrain. *Environmental geology, 47*, 412–420. https://doi.org/10.1007/s00254-004-1166-1

Strahler, A. N. (1957). Quantitative analysis of watershed geomorphology. *American Geophysical Union, Transactions, 38*, 913–920. https://doi.org/10.1029/TR038i006p00913

Strahler, A. N. (1964). Quantitative geomorphology of drainage basin and channel networks. In V. T. Chow (Ed.), Handbook of applied hydrology (pp. 4–76), New York, NY: McGraw Hill Book Co.

Thomas, J., Joseph, S., Thrivikramji, K., Abe, G., & Kannan, N. (2012). Morphometrical analysis of two tropical mountain river basins of contrasting environmental settings, the southern Western Ghats, India. *Environmental Earth Sciences, 66*(8), 2353–2366. https://doi.org/10.1007/s12665-011-1457-2

Topographical Map (79A/3 and 79A/7). (n.d.). Survey of India (SOI), Kolkata, India.